

Coordinated cellular behavior regulated by epinephrine neurotransmitters in the nerveless placozoa

Received: 10 January 2024

Minjun Jin^{1,2,3,4}, Wanqing Li^{1,2,3,4}, Zhongyu Ji^{1,3}, Guotao Di^{1,3}, Meng Yuan^{1,3}, Yifan Zhang^{1,3}, Yunsi Kang^{1,3} & Chengtian Zhao  

Accepted: 25 September 2024

Published online: 04 October 2024

 Check for updates

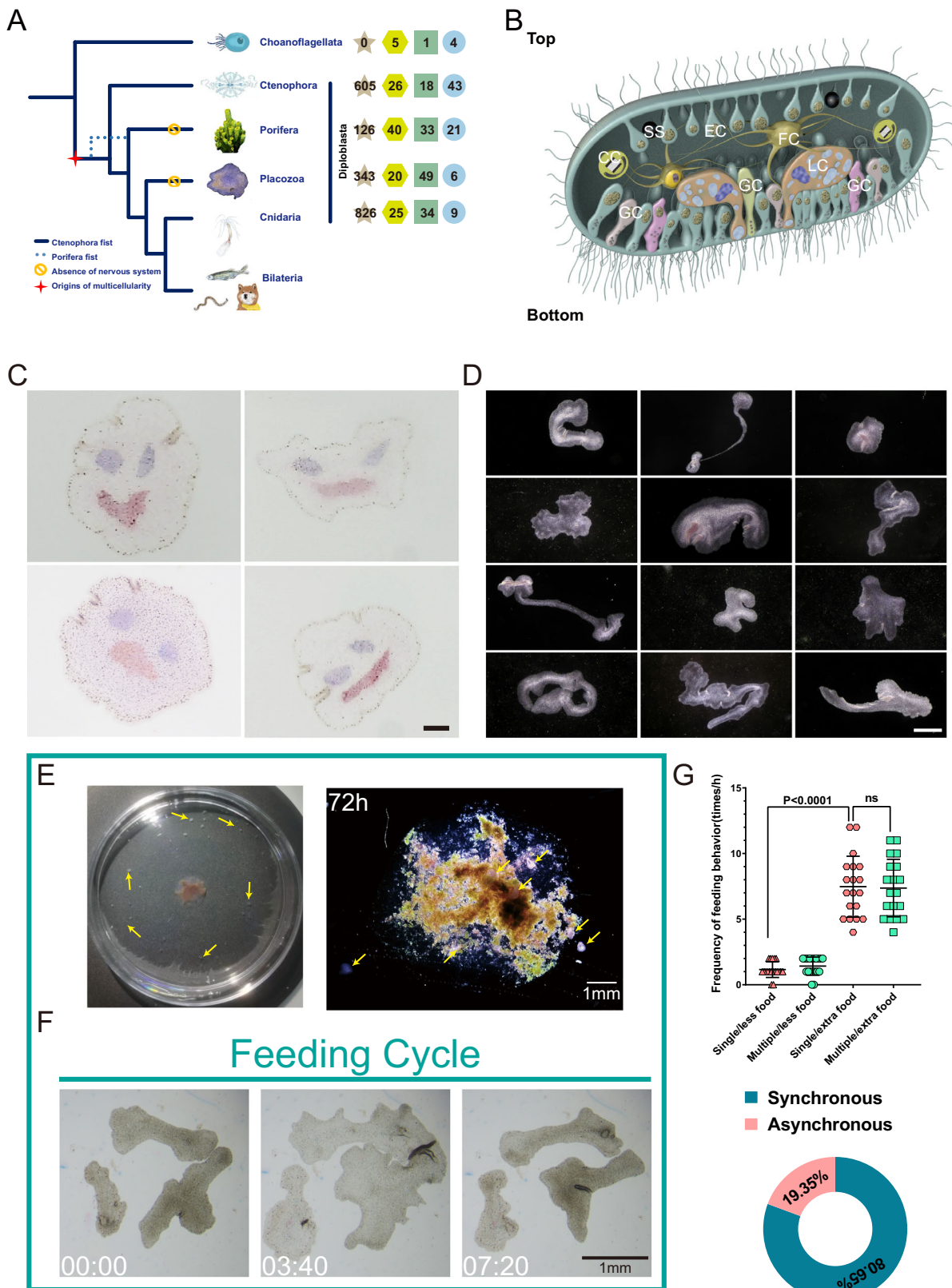
Understanding how cells communicated before the evolution of nervous systems in early metazoans is key to unraveling the origins of multicellular life. We focused on *Trichoplax adhaerens*, one of the earliest multicellular animals, to explore this question. Through screening a small compound library targeting G protein-coupled receptors (GPCRs), we found that *Trichoplax* exhibits distinctive rotational movements when exposed to epinephrine. Further studies suggested that, akin to those in humans, this basal organism also utilizes adrenergic signals to regulate its negative taxis behavior, with the downstream signaling pathway being more straightforward and efficient. Mechanistically, the binding of ligands activates downstream calcium signaling, subsequently modulating ciliary redox signals. This process ultimately regulates the beating direction of cilia, governing the coordinated movement of the organism. Our findings not only highlight the enduring presence of adrenergic signaling in stress responses during evolution but also underscore the importance of early metazoan expansion of GPCR families. This amplification empowers us with the ability to sense external cues and modulate cellular communication effectively.

In single-celled organisms (such as protozoa), the movements often rely on either the beating of motile cilia (ciliates) or the organization of pseudopodia (Amoebozoa). Communication between individuals is relatively less extensive in these cases. In contrast, all the cells are present in a precisely controlled microenvironment in the multicellular organisms and each one needs to detect and respond to cues from their environment. These cues, or cell signals, are generated through cell-cell communication, which is not only essential for the proper functioning of individual cells but also allows the coordinated cellular behavior among groups of cells^{1,2}. In vertebrates, the nervous system typically controls coordinated cellular behaviors, such as locomotion. It remains an enigma of how coordinated cellular behavior is regulated in the basal metazoan before the successful evolution of the central

nervous system or even neurons, which will certainly help us to find clues of how multicellular organisms evolved from a group of single-celled organisms.

The emergence of the nervous system marks a significant milestone in the evolutionary history of life^{3,4}. Traditionally, four phyla (Placozoa, Porifera, Cnidaria, and Ctenophora) are classified as early diverging metazoans (Fig. 1A). Recent chromosome and gene linkage analyses have revealed that ctenophores are the sister group to all other animals^{5–7}. Interestingly, ctenophores evolved a unique nerve net that is fundamentally different from the nervous networks found in cnidarians and bilaterians. It is hypothesized that the nervous system may have evolved independently in ctenophores and cnidarians/bilaterians^{8–10}. Noticeably, both Placozoa and Porifera lack neurons,

¹Fang Zongxi Center, MoE Key Laboratory of Marine Genetics and Breeding, and Institute of Evolution & Marine Biodiversity, Ocean University of China, Qingdao, China. ²Laboratory for Marine Biology and Biotechnology, Qingdao Marine Science and Technology Center, Qingdao, China. ³MoE Key Laboratory of Evolution & Marine Biodiversity, College of Marine Life Sciences, Ocean University of China, Qingdao, China. ⁴These authors contributed equally: Minjun Jin, Wanqing Li.  e-mail: chengtian_zhao@ouc.edu.cn



and some researchers propose that the neural cell types may have been lost during evolution^{5,11}. Remarkably, despite lacking neurons, both Placozoa and Porifera demonstrate complex behaviors under specific conditions. For instance, sponges exhibit “deflation” movements upon sensing amino acids¹², while the placozoan *Trichoplax* exhibits social feeding behavior¹³.

Trichoplax adhaerens, the first identified species within the phylum Placozoa, possesses one of the simplest known body plans^{14,15}. It is primarily composed of six distinct cell types, including an upper and lower layer of ciliated epithelial cells and a middle layer of fiber cells that form connections with multiple cells (Fig. 1B)¹⁶. Among the six cell types, lipophilic cells and gland cells play important roles as secretory

Fig. 1 | Coordinated and uncoordinated cellular movement in *Trichoplax*.

A Phylogenetic tree of the main animal groups and GPCR family classification of pre-bilaterian animals. The number of receptors in each family of GPCRs is shown on the right^{57–59}. Brown: Rhodopsin family; Yellow, Adhesion family; Green, Glutamate family; Blue, Frizzled family. **B** Diagram showing the structure of *Trichoplax*. SS, shiny sphere; EC, epithelial cell; GC, gland cell; CC, Crystal cell; LC, lipophilic cell; FC, fiber cell. **C** Representative images showing different morphology of the same individual stained with bright cresol blue and neutral red at three distinct regions. The movement of this individual was shown in Supplementary Movie 1. **D** Phenotypic diversity of *Trichoplax adhaerens*. **E** Chemotaxis analysis of *Trichoplax*. The left image shows the initial distribution of approximately 20 individuals in

the 5 mm petri dish. The right image shows the accumulation of *Trichoplax* (arrows) near the algae food 72 h later, $N = 3$ independent experiments. **F** Representative images showing the synchronized crinkling and flattening morphology of three individuals when they encounter each other. Their movements are shown in Supplementary Movie 2. **G** Frequency of feeding behavior of *Trichoplax* cultured in less or extra food conditions. “Single” indicates that each individual was cultured separately, while “Multiple” refers to groups of animals cultured together. ns, not significant, Unpaired Mann-Whitney-test. Bottom: percentages of time spent in synchronized versus asynchronous feeding behavior among animals cultured together. $N = 3$ independent experiments. Source data are provided as a Source Data file. 100 μ m in panel (C); 500 μ m in panel (D) and 1 mm in panel (E and F).

cells, with the ability to release lipophilic granules and enzymes that aid in the external digestion of algae^{16,17}. Another noteworthy cell type is the crystal cells, which contain calcium carbonate crystals and are believed to have gravity-sensing capabilities¹⁸.

In addition, *Trichoplax* harbors other unidentified functional cells, including those characterized by shiny spheres (Fig. 1B)¹⁹. It is conceivable that *Trichoplax* may possess additional cell types that require further investigation^{14,19,20}. For instance, a recent study with phylogenetics and comparative single-cell genomics shows that even the peptidergic gland cells contain multiple sub-cell types capable of expressing genes associated with neuronal pre-synaptic activity, reminding the key events in neuronal development²¹.

One of the typical features of *Trichoplax* is the lack of a nervous system, resulting in different parts of the animals moving relatively independently. Interestingly, *Trichoplax* also demonstrates coordinated cellular movement, and this coordination gradually decreases as the animals grow in size. This suggests an intriguing trade-off between cell movement and body size²². Coordinated cell movement is essential in certain situations. For example, when searching for food, *Trichoplax* exhibits chemotaxis, where all its cells can coordinate their movement towards the food source^{23,24}. The feeding behavior may be regulated by peptidergic signaling, as treatments of *Trichoplax* with several peptides can induce the contractility and movements of the animals, resembling feeding behavior^{17,25,26}. Moreover, the epithelial cells display ultrafast contractility, which may facilitate both locomotion and feeding²⁷. It remains an enigma how cells coordinate with each other during synchronized movement in *Trichoplax*.

In this study, through screening compounds targeting GPCR proteins, we demonstrated that epinephrine, a neurotransmitter commonly associated with the fight-or-flight response in vertebrates, participates in the regulation of coordinated cell movement in animals. Despite the absence of conventional neural systems, *Trichoplax* intriguingly employs a unique signaling pathway downstream of epinephrine to govern synchronized cellular motions effectively. Our findings not only highlight the evolutionarily conserved role of epinephrine in stress responses of the metazoans but also reveal distinct regulatory mechanisms at play.

Results

Trichoplax exhibits both coordinated and uncoordinated cellular movements

Although *Trichoplax* is a simple organism mainly consisting of two thin layers of cells, it exhibits remarkably dynamic and complex cellular movements. To provide a clearer depiction of this phenomenon, we randomly marked three regions of the organism, allowing us to monitor gross morphology over time. Notably, in addition to overall changes, the shape of each labeled region can readily shift, implying that these three labeled regions constantly manifest distinct movement patterns (Fig. 1C and Supplementary Movie 1). Consequently, each part of the organism can move relatively independently, leading to the formation of diverse morphologies (Fig. 1D).

Intriguingly, *Trichoplax* also demonstrates synchronized cellular movement. For instance, as previously reported, these organisms

exhibit a pronounced tendency to move toward food sources^{23,24}. When placed randomly in the culture dishes, around 35% of the animals ($n = 60$) accumulated on the algal agarose located in the central region 72 hours later (Fig. 1E). Interestingly, when multiple individuals encounter one another, they display synchronized feeding behaviors characterized by alternating flattening and crinkling motions (Fig. 1F, G and Supplementary Movie 2). Noticeably, these behaviors are synchronized only when two animals are in close proximity and become asynchronous once they separate (Supplementary Movie 2). In addition, the feeding frequency remains similar between single and grouped individuals, but it significantly changed with the amount of food supplied (Fig. 1G). Overall, these findings suggest that coordinated and synchronized cellular movements occur both within individual *Trichoplax* and among different individuals. This raises the question: how do these organisms regulate coordinated cellular movement in the absence of a nervous system?

Response of *Trichoplax* to different compounds targeting GPCRs

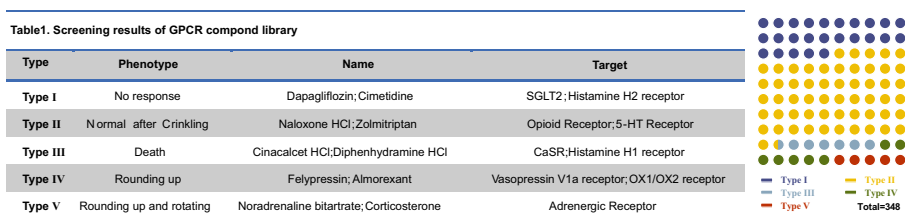
The coordinated cellular movements require the communication between diverse cells. In vertebrates, GPCRs are essential molecules that play a large variety of functions during cell communication. Interestingly, while GPCRs are rarely observed in single-celled organisms, they exhibit significant expansion in the basal metazoans, particularly within the rhodopsin GPCR family (Fig. 1A). It is plausible that these GPCRs fulfill important roles in cell-cell communication with the evolution of multicellular organisms. Considering this, we performed a small compound library screening with 348 compounds targeting GPCRs.

By adding these compounds directly into the medium containing *Trichoplax* and following with behavior analyses, we observed five types of behaviors after treatments (Fig. 2). About 87 compounds had no detectable effects on the movement of *Trichoplax* (Type I, Fig. 2). Most of the compounds (196 out of 348) induced the initial crinkling at 2 min after treatments, while the animals changed to normal movements shortly (Type II, Fig. 2). Treatments of 24 compounds resulted in final death of the animals (Type III, Fig. 2). Some compounds caused rounding of the animals without clearly movement (Type IV, Fig. 2). Interestingly, we found 17 compounds caused animal rounding and then followed by in situ rotational movements (Type V, Fig. 2). Strikingly, most of these 17 compounds are listed as targeting compounds for the adrenergic receptors (Supplementary Data 1).

Rotational movement of *Trichoplax* after epinephrine treatments

The screening results suggested that adrenergic signals may participate in the regulation of rotational movements of *Trichoplax*, promoting us to further test the role of epinephrine on placozoa movements. We introduced epinephrine directly to the culture medium containing *Trichoplax*. Following the treatment, the animals were transiently crinkled and then exhibited a nearly circular shape at ~2.5 mins post-treatment (Fig. 3A, B and Supplementary Movie 3). We observed sustained rotational movement in the treated animals for an

A



B

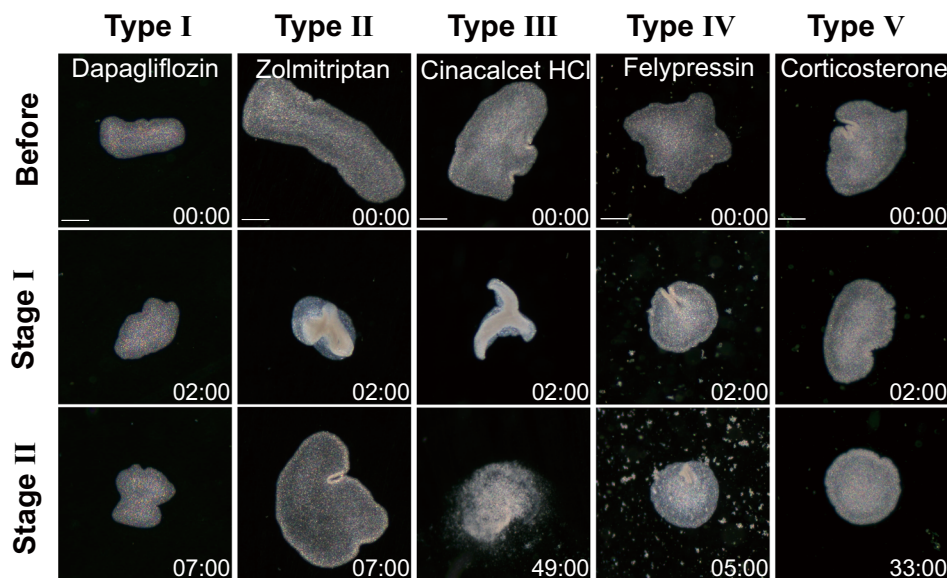


Fig. 2 | Small molecular screening in *Trichoplax*. A Screening results showing the typical phenotype and compounds in each group. The relative number of compounds in each group is shown on the right. B Representative images showing the

phenotypes of the animals treated with different types of drugs at different time points as indicated. Time, min: sec. Scale bars, 100 μ m.

extended duration ranging from several minutes to over one hour. Further analysis on circularity and surface area showed that the animals changed their shapes from irregular to circular after treatments (Fig. 3C). Moreover, the trajectories of the individual cells on the edge sides of the organisms exhibited a circular movement pattern, in contrast to the random pattern observed in control animals (Fig. 3D). The rhythmic circular movement was further demonstrated by measuring the angles of the animals, which showed that the epinephrine treatment caused the rotational movements of the animals at a frequency of ~2 Hz (2 rotations per minute) (Fig. 3E). The average velocity of individual cells, as measured by the moving distance of the edge, was also significantly increased after treatment (Fig. 3F). Finally, we recorded the trajectories of the animals during a one-hour treatment with a lower concentration of epinephrine, which showed that the treated groups displayed a tendency towards localized circular movement (Fig. 3G). Together, these results confirmed our screening results and demonstrated that epinephrine treatments can cause rotational locomotion of *Trichoplax*.

Epinephrine is a small-molecule neurotransmitter that is widely utilized in vertebrates. With the emergence of multicellular animals, small molecule neurotransmitters have also evolved to mediate cell-cell communication^{28,29}. For example, nitric oxide (NO) has been shown to regulate cilia activity in ctenophores, while L-glutamate, glycine, and GABA are involved in regulating feeding behavior in placozoa^{30,31}. We further asked whether the rotational movement observed in *Trichoplax* is a specific effect of epinephrine or a general response to neurotransmitter stimulation. To address this, we further

treated *Trichoplax* with several small molecule neurotransmitters, including Glycine, Serotonin (5-HT), Histamine, Acetylcholine (Ach), Tyramine, GABA, and Dopamine. Treatments with Tyramine, Histamine, or 5-HT caused crinkling of the placozoa, and prolonged exposure or high concentration of these neurotransmitters ultimately led to animal death (Supplementary Fig. 1, Supplementary Movies 4 and Supplementary Data 2). In contrast, incubation with Glycine, Ach, or GABA had minimal effects on the animal's shape (Supplementary Fig. 2, Supplementary Movies 5 and Supplementary Data 2).

As previously reported, the higher concentration of glycine (10 mM/L) also resulted in animal death³⁰. Interestingly, dopamine treatment caused the animals to assume a rounded shape (Supplementary Fig. 2D and Supplementary Movie 5). We further treated the animals with octopamine, a common catecholamine frequently used in invertebrates²⁹. The treated animals did not exhibit any noticeable rotational movements (Supplementary Fig. 3). Altogether, none of these neurotransmitter treatments induced rotational movement in the placozoa (Summarized in Supplementary Data 2). In contrast, treatments with epinephrine analogs such as Isoprenaline and Methoxamine can induce rotational movements (Supplementary Fig. 3 and Supplementary Movies 6). These results provide strong evidence that the rotational behaviors exhibited by the animals are specific responses to epinephrine signals, distinguishing them from other neurotransmitters.

Identification of potential adrenergic receptors in *Trichoplax*
We hypothesize that epinephrine is more likely to regulate coordinated cilia beating via the adrenergic receptors. By searching the

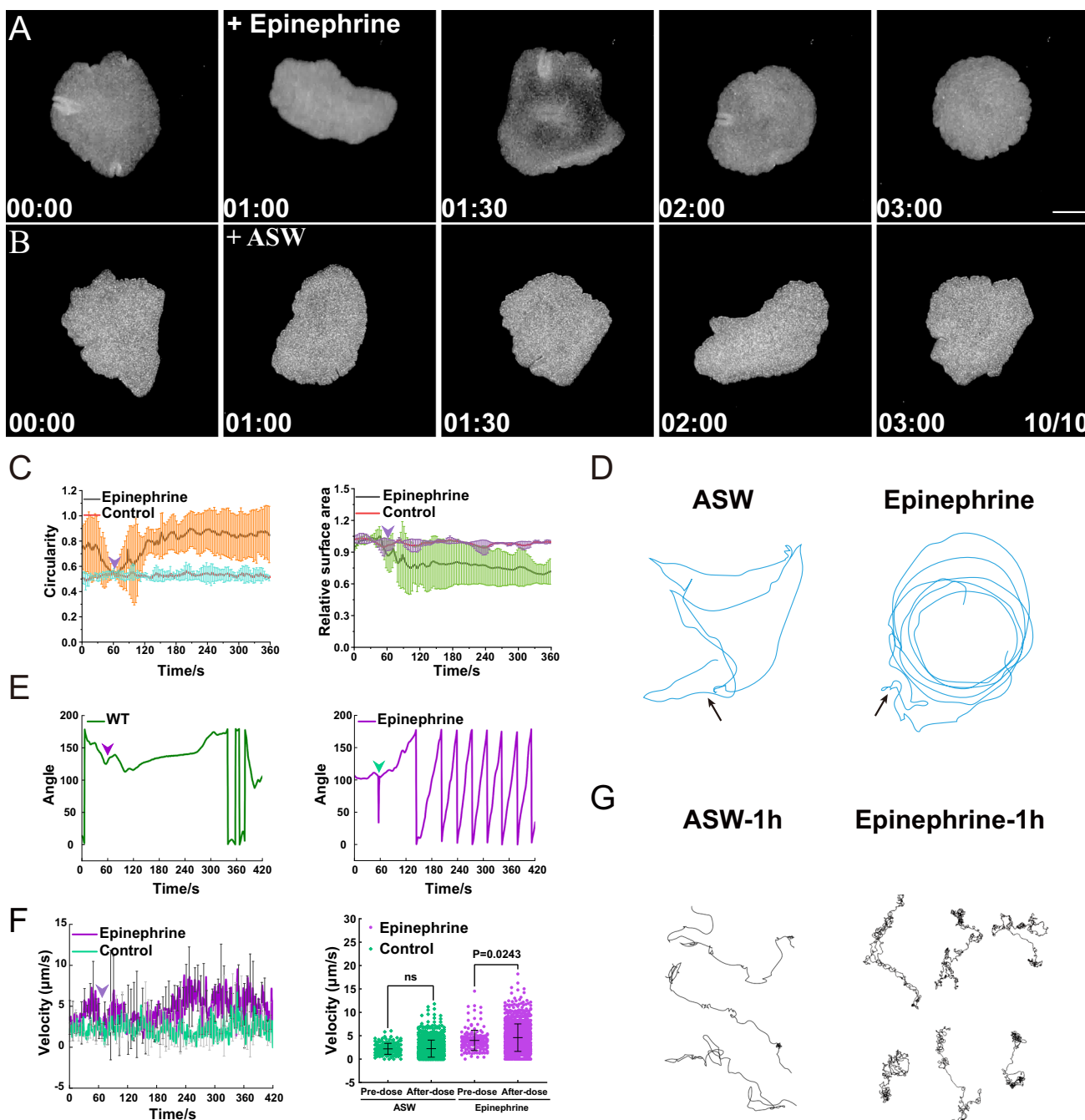


Fig. 3 | Rotational movement of placozoa in response to Epinephrine treatments. **A, B** Phenotypes of *Trichoplax* treated with epinephrine (**A**) or ASW (artificial seawater) (**B**) at different time points as indicated. **C** Statistical results showing the circularity and relative surface area of the animals in ASW or epinephrine-treated groups. Data are presented as mean \pm SE, $N = 3$ independent experiments. **D** Motion trajectories of the animals in ASW or epinephrine-treated groups, with arrows indicating the position of *Trichoplax* at the time of administration.

E Changes of body directional angle in ASW or epinephrine-treated groups. **F** Velocity of individual cells in the animals of ASW or epinephrine treated groups. Data are presented as mean \pm SE, $N = 3$ independent experiments. Unpaired Mann-Whitney-test. Source data are provided as a Source Data file. **G** Motion trajectories of the animals treated with ASW or low concentration of epinephrine for one hour. Scale bars, 100 μ m.

T. adhaerens genome, we identified six candidate adrenergic receptor-like proteins, and homologs of these receptors were also present in other basal metazoans (Supplementary Fig. 4). By plotting several published RNA-seq transcriptome database^{31–33}, we found that *Tad_60482* and *Tad_60646* exhibited relatively higher expression level in *Trichoplax* (Supplementary Fig. 5A). Further real-time quantitative PCR (qPCR) analysis proved that *Tad_60482*, *Tad_60646*, *Tad_3759* and *Tad_61720* are expressed at a higher level than other genes in *Trichoplax* (Fig. 4A).

Next, we conducted RNA interference (RNAi) experiments targeting each of these genes. We applied a gene knockdown strategy based on spike silica nanoparticles (SSN)-mediated RNAi approach^{34–36}. These silica nanoparticles contain virus-mimetic spikes that are positively charged. Upon incubation with siRNA/shRNA, these spikes have the ability to bind to siRNA/shRNA molecules and facilitate their transportation into cells through docking and endocytosis, resembling the mechanism employed by coronaviruses (Supplementary Fig. 5B)³⁴. With this approach, we were able to knockdown the expression of

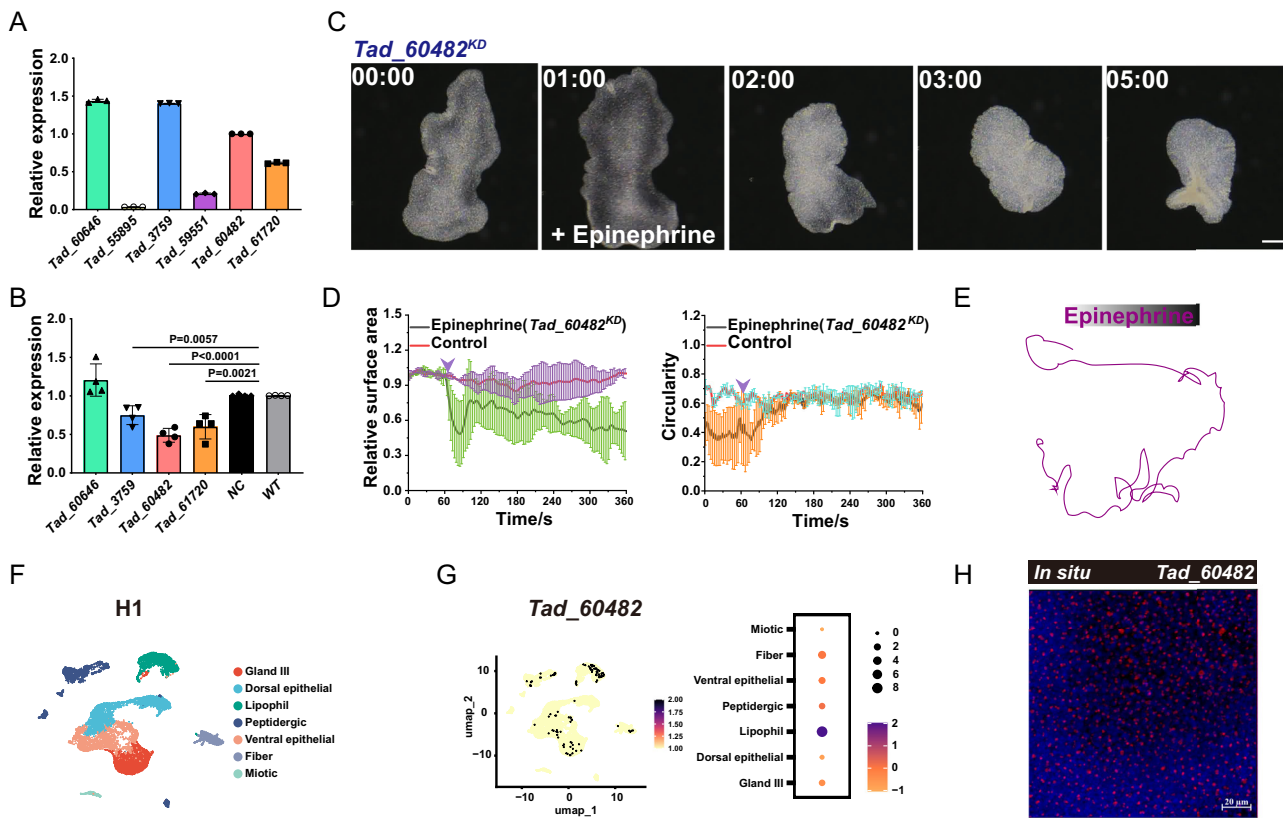


Fig. 4 | Identification of the major adrenergic receptors. **A** qPCR results showing the expression of potential adrenergic receptors in *Trichoplax*, $N=3$ independent experiments. The graphs shown represent the mean \pm SD of independent experimental replicates. **B** qPCR results show the expression of potential adrenergic receptors following shRNA knockdown. For each gene, the expression level of wild-type animals was set as 100%. NC, non-target control shRNA. WT, wild-type animals. $N=4$ independent experiments. The graphs shown represent the mean \pm SD of independent experimental replicates. two-tailed Unpaired *t* test. **C–E** Phenotypic analysis showing the motion behavior of the animals treated with *Tad_60482*

shRNA. Data are presented as mean \pm SE, $N=3$ independent experiments. Source data are provided as a Source Data file. **F** Unsupervised UMAP of scRNA-seq dataset (Accession number: 10.17632/bbpkbx968s.2) from *Trichoplax adhaerens* (H1) showing the cluster of different cell types as indicated. **G** Gene expression pattern of *Tad_60482* on different cell types from scRNA-seq data. Relative expression level in different clusters is shown on the right. **H** FISH results show the expression of *Tad_60482* in multiple cells. Scale bars, The same results were obtained in three independent experimental replicates. 100 μ m in panel (C) and 20 μ m in panel (H).

these adrenergic receptor-like genes (Fig. 4B). With the exception of *Tad_60646*, the expression levels of *Tad_60482*, *Tad_3759* and *Tad_61720* showed significant downregulation in the treated groups (Fig. 4B). Subsequently, we treated the knockdown groups with epinephrine and observed that the rotational movement was largely preserved in the *Tad_60646*, *Tad_3759* and *Tad_61720* knockdown groups (Supplementary Fig. 5C). Interestingly, the rotational movement was significantly diminished when gene *Tad_60482* was knocked down (Fig. 4C–E).

Notably, the circularity of the *Tad_60482* knockdown animals resembled that of the untreated control, in contrast to the increased circularity observed in the other groups (Fig. 4D and Supplementary Fig. 5C). Furthermore, we performed a knockdown analysis of *Tad_60482* using a commercial transfection reagent, FuGENE6, which has been successfully used for gene silencing in placozoa³⁷. Similarly, the rotational movement upon epinephrine treatment was greatly inhibited in the knockdown animals (Supplementary Fig. 5D–F). Thus, both gene silencing methods suggest that *Tad_60482* encodes the major receptors for epinephrine signaling in *Trichoplax*.

To explore which cell types are capable of expressing the *Tad_60482* gene, we plotted a recently published single-cell transcriptome database²¹. The results indicated that *Tad_60482* exhibited a broad expression profile across various cell types, encompassing lipophilic cells, gland cells, and epithelial cells (Fig. 4F, G). The wide expression pattern of this adrenergic receptor was further validated through *in situ* hybridization of *Tad_60482* (Fig. 4H). Thus, while we

cannot completely exclude the involvement of other potential receptors, including *Tad_60646*, our findings strongly suggest that *Tad_60482* plays a significant role in the regulation of rotational movement in *Trichoplax* following epinephrine treatments.

Calcium and redox signaling function downstream of adrenergic receptors to regulate coordinated ciliary movement

We aimed to identify the primary signaling pathway that controls the epinephrine-regulated rotational movements. In vertebrates, calcium and cAMP are two major intracellular signals that regulate cellular physiology downstream of adrenergic receptors. To investigate their potential involvement, we first examined the effects of Forskolin and Caffeine, two commonly used cAMP-elevating drugs in vertebrates, on the movement of *Trichoplax*. Upon treatment, the animals either displayed no response or exhibited crinkling at high concentrations of these chemicals (Supplementary Fig. 6A, B, and Supplementary Movies 7). Furthermore, supplementing the medium with cAMP had no impact on the movement of the organisms (Supplementary Fig. 6C and Supplementary Movie 7).

Next, we incubated *Trichoplax* in seawater with low concentrations of calcium and magnesium. After short-term incubation, the organisms' movement slowed down while still maintaining their regular shape. Strikingly, the rotational movement of the animals was completely blocked after epinephrine treatments (Supplementary Fig. 7 and Supplementary Movies 8). Similarly, the use of EGTA to chelate intracellular calcium ions also resulted in the blockade of

epinephrine-regulated rotational movements (Fig. 5A–C and Supplementary Movies 8). Altogether, although we cannot exclude the involvement of cAMP in the rotational movements due to the potential non-functionality of Forskolin and Caffeine, our findings suggest that calcium signaling plays a vital role in regulating rotational movements in *Trichoplax* following epinephrine treatments.

Being a basal metazoan without muscle and neuronal cells, the placozoa moves primarily by means of cilia in the ventral epithelia (Fig. 1B). Using high-speed video microscopy, we further analyzed the ciliary beating pattern. In the absence of epinephrine, the cilia typically exhibited beating patterns in various directions, corresponding to the random movements observed in the animals (Fig. 5D, E and Supplementary Movie 9). In contrast, following the rotational movements of the animal after treatments, most cilia beat in the same direction (Fig. 5D, E and Supplementary Movie 9). These results suggested that epinephrine treatments can regulate the beating direction of cilia, thus the movement of *Trichoplax*. We have shown previously that redox signals are essential for the coordinated movements of cilia in both *Chlamydomonas* and zebrafish³⁸.

To further investigate the requirement of redox signals for the coordinated ciliary beating in the placozoa, we treated the animals with several compounds regulating the redox signaling pathway. Although treatments with oxidants such as T-booth and hydrogen peroxide did not elicit a noticeable response in the movements of the animals at lower concentrations, these treatments were able to completely inhibit the rotational movements induced by epinephrine activation (Supplementary Fig. 8A). Similarly, increasing the reduced state using compounds like Tempol or dithiothreitol (DTT) also inhibited the epinephrine-regulated rotational movements (Supplementary Fig. 8A).

The redox state of the cilia is at least partially regulated by CYB5D1 protein through its heme binding activity³⁸. We found placozoa also possesses a CYB5D1 homolog with a high degree of conservation (Supplementary Fig. 8B). Knockdown of *Tad_cyb5d1* has relatively minor effects on the movement of *Trichoplax*, while the rotational effects of epinephrine treatments were significantly diminished in these knockdown animals (Fig. 5F–I and Supplementary Movie 10). Together, these data demonstrated that calcium and ciliary redox signaling mediated the epinephrine-induced coordinated cellular movement in *Trichoplax*.

Evolutionary conserved roles of epinephrine in placozoa

Finally, we sought to determine the physiological functions of the coordinated cilia beating upon epinephrine treatments. We first examined whether endogenous epinephrine signals were indeed present in *Trichoplax*. By enzyme-linked immunosorbent assay (ELISA), we confirmed that adrenergic signals are present in the cellular lysis of *Trichoplax* to activate alpha-adrenergic receptors (Fig. 6A). In humans, epinephrine is a well-known hormone involved in the body's stress response. We postulated that epinephrine may play similar roles in *Trichoplax*. To test this hypothesis, we designed an electric shock device by putting the positive and negative electrodes next to the animals (Fig. 6B). By giving a small amount of shock, we noticed that the animals initially displayed rotational movements and then gradually moved away from the shock center, similar to those treated with low concentrations of epinephrine. (Figs. 6C, D, 3G and Supplementary Movie 11). Notably, the concentration of adrenergic signals was significantly increased after electric shock (Fig. 6E). These results suggest that adrenergic signals are released in response to electric shock, directing the animals to exhibit negative taxi behavior.

The rotational movement of the animals following epinephrine treatments could be attributed to the direct addition of epinephrine to the culture medium, saturating the surrounding environment with epinephrine signals. Notably, when we introduced a small quantity of epinephrine exclusively to one side of the animal, we observed a rapid

negative taxi behavior from the injection area (Fig. 6F and Supplementary Movie 12). These findings strongly support the notion that the basal metazoan *Trichoplax* may employ epinephrine as a negative taxi signal to modulate their cellular behavior, similar to the role of epinephrine in stress responses of vertebrates.

Treatment of unicellular organisms with epinephrine

Since epinephrine can regulate the negative taxis behavior of placozoa, we further asked whether epinephrine can also regulate the swimming behavior in single-celled organisms. We examined the effects of epinephrine on the swimming of *Euplotes vannus*, one of the most complicated ciliated protozoan³⁹. Upon epinephrine treatments, the swimming pattern remained unchanged (Supplementary Fig. 9A). Similarly, the swimming behavior of the unicellular green alga *Chlamydomonas reinhardtii* also showed no response to epinephrine signals (Supplementary Fig. 9B, C). By searching the genomes of *E. vannus* and *C. reinhardtii*, we failed to find any conventional adrenergic receptors. Choanoflagellates are among the closest unicellular relatives of metazoans. Similarly, no adrenergic receptor-like genes are present in the genomes of choanoflagellates. Thus, the roles of epinephrine signals during stress response are more likely to be functional in metazoans.

Discussion

As one of the basal multicellular animals, placozoa lack distinct organs, tissues, or specialized cell types such as neurons or muscles. The cells within these animals appear to have less interconnection, and each cell is capable of movement through simple contractile mechanisms or by using cilia. This individual cell mobility allows the entire animal to exhibit diverse shapes (Fig. 1D). Intriguingly, under specific conditions like locating a food source, all the cells in the organism can move collectively in a coordinated manner. This suggests the presence of a mechanism regulating cell-cell communication to enable such coordinated movements.

In vertebrates, GPCRs play a crucial role in facilitating cell-cell communication, enabling cells to perceive and respond to signals from their extracellular environment. Throughout the course of evolution, from single-celled organisms to multicellular organisms, the GPCR family has undergone significant expansion, concomitant with the evolution of intricate cellular communication mechanisms in multicellular organisms. Considering this, we performed behavioral analysis on *Trichoplax* by screening a GPCR small compound library. Notably, these small compounds were originally designed to target GPCRs in vertebrates. Due to the structural differences between vertebrate and placozoa GPCRs, many compounds were likely to have minimal or no effects on the animals' movements, which was confirmed by our screening results.

Interestingly, our results demonstrated that epinephrine signals are at least conserved in regulating coordinated cellular movements in this nerveless animal. Treating *Trichoplax* with epinephrine induced rotational movement, which could be blocked by knocking down one of the adrenergic receptors. We further showed that calcium and redox signals are also involved in the regulation of rotational movement downstream of adrenergic receptors. Although we cannot rule out the possibility of epinephrine binding to non-adrenergic receptors, our data suggest the presence of an adrenergic signaling pathway in *Trichoplax*. Ligand binding to adrenergic receptors likely enhances intracellular calcium levels, which subsequently modulate ciliary beating through the mediation of redox signals (Fig. 6G). Despite the absence of neuron synapses, the placozoa can still use neurotransmitters such as epinephrine to regulate cell-cell communication directly.

Strikingly, the function of epinephrine signals appears to be exclusive to metazoans, given that unicellular organisms like *Euplotes*, *Chlamydomonas*, and even choanoflagellates lack the

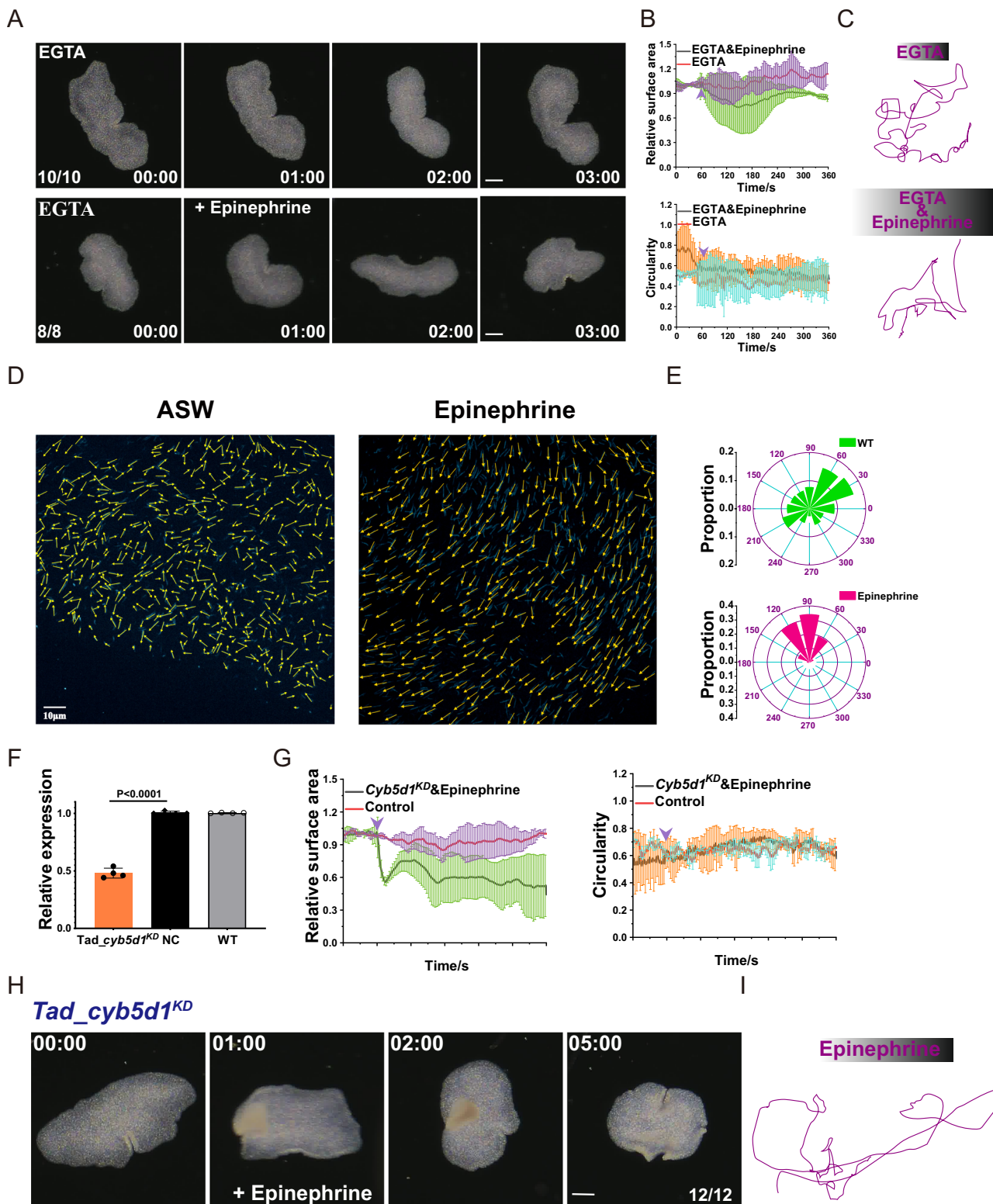


Fig. 5 | Calcium and redox signaling are required for coordinated ciliary movement. **A–C** Phenotypic analysis showing the motion behavior of the animals treated with Epinephrine and EGTA. Data are presented as mean \pm SE, $N=3$ independent experiments. **D** Still images showing the beating directions of cilia in control or epinephrine-treated animals. The same results were obtained in three independent experimental replicates. **E** Angular distribution graph showing the beating direction of individual cilia in control or epinephrine-treated animals.

F qPCR analysis showing the relative expression level of *Tad_cyb5d1* following shRNA knockdown, $N=4$ independent experiments. The graphs shown represent the mean \pm SD of independent experimental replicates. *P*-values were calculated using two-tailed followed by an unpaired *t* test. **G–I** Phenotypic analysis of *Tad_cyb5d1*-knockdown animals following epinephrine treatments. Data are presented as mean \pm SE, $N=3$ independent experiments. Source data are provided as a Source Data file. Scale bars, 100 μ m in Panels (A and H), and 10 μ m in Panel (D).

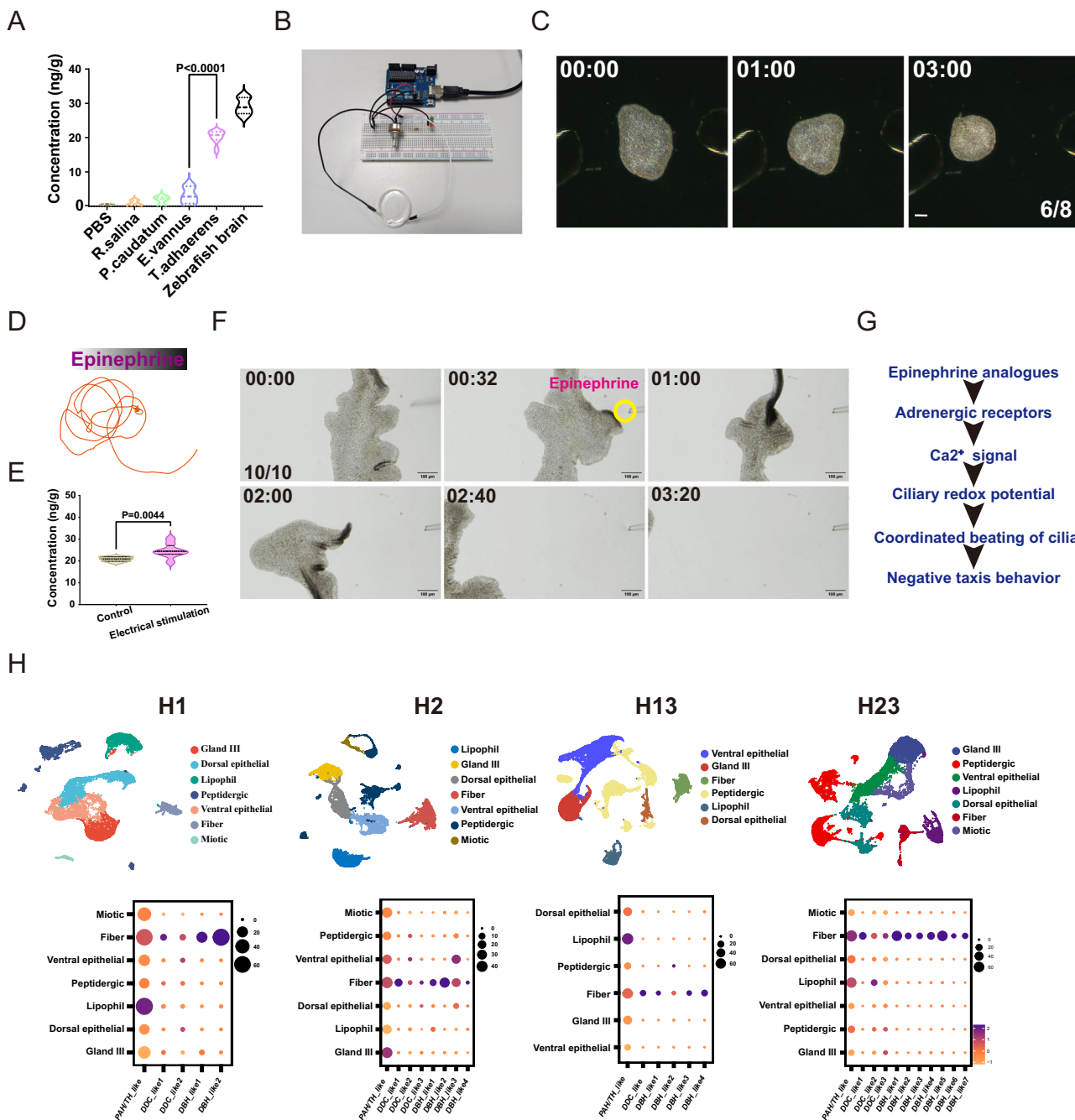


Fig. 6 | Adrenergic signals regulate negative taxi behavior in *Trichoplax*.

A Detection of adrenergic signals through ELISA analysis. PBS solution was used as a negative control, while zebrafish brain extracts were used as a positive control. *R.salina*: *Rhodomonas salina*, *P.caudatum*, *Paramecium caudatum*, *E.vannus*, *Euplates vannus*. two-tailed Unpaired *t* test. B A homemade device for electrical stimulation of *Trichoplax*. C, D The morphology and motion trajectories of *Trichoplax* after electric stimulation. E ELISA analysis shows the increased concentration of adrenergic signals after electric stimulation. Unpaired Mann-Whitney test. F Time-lapse images showing the negative taxi behavior following local

epinephrine stimulation. G A proposed signaling pathway downstream of adrenergic signals regulating negative taxis in *Trichoplax*. H Expression analysis of genes that are potentially involved in the synthesis of adrenergic signals. The top panels show the clusters of different cell types from scRNA-seq analysis in different haplotypes of *Trichoplax* as indicated. The bottom panels show relative gene expression levels in different clusters. The expression of the following genes (H1) was plotted: PAWTH_like: *Tad_32954*; DDC_like1: *Tad_31153*; DDC_like2: *Tad_60611*; DBH_like1: *Tad_55459*; DBH_like2: *Tad_55460*. The homologous genes in other strains were identified using BLAST search. Scale bars, 100 μ m.

conventional adrenergic receptors. In contrast, homologs to adrenergic receptors are present in the genomes of ctenophores and poriferans (Supplementary Fig. 4). It will be interesting to test the effects of epinephrine on the behavior of these basal metazoans. Taken together, our data suggest that the expansion of the GPCR family represents a pivotal breakthrough for multicellular organisms in their endeavor to orchestrate effective cell-cell communication mechanisms.

In addition, it is intriguing to elucidate which specific cell types within *Trichoplax* possess the ability to secrete adrenergic signals. Through exploration of the *Trichoplax* genome, we identified several genes implicated in the synthesis of monoamine neurotransmitters, notably phenylalanine hydroxylase (PAH), dopa decarboxylase (DDC), and dopamine hydroxylases (DBH)-like genes (Supplementary Fig. 10). Remarkably, upon plotting several published single-cell transcriptomes across various haplotypes of placozoa (H1, H2, H13, and

H23^{21,40}, we unveiled a significant enrichment of these genes in fiber cells (Fig. 6H). This unique cell type, characterized by multiple axon-like processes and interactions with other cell types, is involved in the regulation of animal contractility and innate immunity (Fig. 1B)⁴¹. The noteworthy expression of these genes in fiber cells strongly suggests the potential capability to secrete adrenergic signals, thereby regulating cell-cell coordination and animal movements. It remains unclear how fiber cells secrete adrenergic signals to their surrounding cells.

Genomic analysis suggests that essential components for tight junctions are not present in the *Trichoplax* genome, and active zones similar to those in synapses may not form in placozoa^{15,42}. Several recent studies suggest that many cells can send signaling molecules directly to their target cells via a novel filopodium-based structure named cytoneme^{43–46}. A notable feature of fiber cells is the presence of multiple long filopodia connecting neighboring cells (Fig. 1B). It is possible that these adrenergic signals are secreted to target cells via this structure. Actually, essential components for vesicle secretion, including SNAP25 and Synaptotagmin, are expressed in fiber cells (single cell analysis)²¹. Further investigation will be needed to elucidate the underlying mechanism.

Finally, the formation of the monoaminergic system has long been recognized as an innovation for bilaterians⁴⁷. Moreover, *Trichoplax* lacks tyrosine hydroxylase (TH), a pivotal enzyme in catecholamine synthesis^{15,29}. In contrast, our ELISA results intriguingly revealed the presence of bioactive molecules in *Trichoplax* capable of activating adrenergic receptors. We think this molecule belongs to the epinephrine or epinephrine-like transmitter category, while the exact chemical composition of this molecule remains unknown. The unknown structure of this molecule may explain why regular mass spectrometry methods failed to detect the presence of monoamine in basal metazoans²⁹.

This also raises the possibility of the existence of non-canonical or specific enzymes responsible for synthesizing these molecules in basal animals. Moreover, it remains unknown whether this non-canonical pathway is due to convergent evolution specific to placozoa or is also present in other basal metazoans. Interestingly, despite the absence of the TH enzyme, several studies have documented the presence of monoamine molecules in cnidarians^{48–52}. The synthesis pathway of these monoamines in basal metazoans requires further investigation.

In summary, our findings from both local delivery and electric shock experiments strongly support the notion that epinephrine signals can regulate the negative taxi behavior of placozoa, akin to their role as fight-or-flight neurotransmitters in humans. The expansion of GPCR families has bestowed multicellular organisms with remarkable capabilities to perceive external signals and modulate cell-cell communication, representing a significant advancement in their evolutionary development.

Methods

Ethics statement

This study involved the use of single-cell organisms and *Trichoplax adhaerens*, which are not subject to animal welfare regulations because they lack complex nervous systems. All zebrafish studies were conducted according to standard animal guidelines and approved by the Animal Care Committee of the Ocean University of China (OUC2012316).

Animals

Trichoplax adhaerens were obtained from Drs. Leo Buss and Carolyn L. Smith and maintained in the natural seawater of Qingdao (pH 8.25, 30 ppt). We grew *T. adhaerens* in glass Petri dishes (200 mm diameter and 30 mm high) with 200 ml of sterilized natural seawater at constant and controlled temperature (23 °C) and humidity (60%)

with a photoperiod of 14 h/10 h light/dark cycle in an environmental chamber (Ningbo Jiangnan RXZ-B). *T. adhaerens* were fed with red algae (*Rhodomonas salina*).

Chemotactic analysis

For chemotaxis assays, algae were concentrated by centrifugation and suspended in low melting-point agarose (~10⁶ cells/10 µL). We dropped 300 µL of low-melting-point agarose containing algae in the center of a 5 mm petri dish. After the agar cooled and solidified, 20 mL of ASW was added. The dish was kept at room temperature for 1–2 hours. About twenty *Trichoplax* were placed at varying distances from the algae pellet in the dish. The temperature was maintained at 25 °C, and pictures were taken after three days.

Cell movement analysis

We used bright cresol blue and neutral red to label different parts of the *Trichoplax* and placed the labeled *Trichoplax* in 3.5 mm petri dishes. The behavior of the animals was recorded using WT-1000GM software under a Zeiss stereomicroscope (Stemi 508) equipped with a CCD camera (Weitu HD200C). Time-lapse images were recorded at 1-second intervals.

Pharmaceutical treatments

The GPCR compound library was purchased from Target Molecule Corporation (L1500). Thirty minutes prior to treatment, the animals were transferred from culture Petri dishes to confocal Petri dishes containing 1 ml of ASW (11 mM CaCl₂, 10 mM KCl, 40 mM MgCl₂, 15 mM MgSO₄, 435 mM NaCl, 2.5 mM NaHCO₃, 7 mM Tris base and 13 mM Tris-HCl). Once the animals acclimated to the new environment, we removed excess liquid, resulting in a volume of 400 µL. Next, we dissolved 2.5 µL of each compound in 100 µL of ASW and added them to the Petri dishes, achieving a final concentration of 50 µM for each compound. The behavior of the animals was recorded using WT-1000GM software under a Zeiss stereomicroscope (Stemi 508) equipped with a CCD camera (Weitu HD200C). Time-lapse images were recorded for at least 7 min (1 min before adding the sample to 6 min after sampling) at 1-second intervals. The experiments were repeated at least three times for each drug. For behavioral analysis of the animals in low concentrations of calcium and magnesium (LCM-ASW), these experiments were repeated with ASW containing 0.55 mM Ca²⁺ and 2.775 mM Mg²⁺. The behavioral analysis of the animals following treatments with various neurotransmitters—glycine, serotonin (5-HT), histamine, acetylcholine (Ach), tyramine, GABA, and dopamine—was conducted in a similar manner. In most cases, we treated the animals with both high and low concentrations (Supplementary Data 2). The typical concentrations for behavior analysis are as follows: Epinephrine (60 mM), Supplementary Fig. 1: Tyramine (10 mM), Histamine (1 mM), 5-HT (10 mM); Supplementary Fig. 2: Glycine (1 mM), Acetylcholine (10 mM), GABA (30 mM) and Dopamine (30 mM); Supplementary Fig. 3 Isoprenaline (100 mM), Methoxamine (10 mM) and Octopamine (120 mM); Supplementary Fig. 6: Forskolin (1 mM), Caffeine (20 mM) or cAMP (0.1 mM).

Behavior analysis

For analyzing the behavior of the animals after drug treatments, we primarily utilized the ImageJ program. Briefly, the time-lapse sequences of the *Trichoplax* movement were imported into the Fiji ImageJ software. First, we analyzed the area and roundness of the animals. Subsequently, the animals' positions and motion paths were determined using the MTrack2 and Manual Tracking plugins, respectively. The motion angle was measured using the (PAT-GEOM v1.0) plugin⁵³. The velocity of the animals was assessed by measuring the distance moved by a fixed cell on the edge. All behavioral data, including area, roundness, trajectory, velocity, and angle, were subjected to analysis using GraphPad Prism 9. All experiments were repeated at least three times.

Identification of potential adrenergic receptors and genes involved in monoamine synthesis

For identification of potential adrenergic receptors, we first used the human adrenergic receptor gene (ID number: P35348/P35368/P25100/P08913/P18089/P18825/P08588/P07550/P13945) to BLAST candidate genes within the basal metazoans. This included species such as *Nematostella vectensis* (GCF_932526225.1), *Amphimedon queenslandica* (GCF_000090795.2), *Mnemiopsis leidyi* (AGCP000000000), *Trichoplax adhaerens* (ABGP000000000), *Euplotes vannus* (EVDB, <http://evan.ciliate.org>), *Chlamydomonas reinhardtii* (GCF_000002595.2), *Monosiga brevicollis* (GCF_000002865.3), *Salpingoeca rosetta* (GCF_000188695.1). Genes with BLAST alignment E-values less than $1e^{-5}$ were selected as candidates. We then further BLASTed these hits against the human genome to eliminate genes whose top five hits did not include adrenergic receptor genes. Additionally, we used human Frizzled family genes, another GPCR family, as the outgroup for phylogenetic analysis. The protein sequences were aligned using MAFFT⁵⁴. Mega 11 was used to construct the maximum likelihood and Bayesian phylogenetic trees. The Maximum Likelihood Tree's robustness was tested with 1000 ultrafast bootstrap replicates. Trees were visualized and annotated in Adobe Illustrator. Similarly, human genes related to monoamine synthesis, including DBH (ID:NP_000778.3), DDC (ID:NP_000781.2), PAH (ID:NP_000268.1), and TH (ID:NP_000351.2), were used to blast candidate genes within basal metazoans. The identified genes were further blasted back to the human genome database to eliminate false orthologues. The Maximum Likelihood Tree's robustness was tested with 1000 ultrafast bootstrap replicates. Finally, the maximum likelihood method was used to construct the phylogenetic tree.

Fluorescence in situ hybridization

For fluorescence in situ hybridization (FISH) analysis, we used the π -FISH rainbow method as previously discussed⁵⁵. All the probes and detection reagents were purchased from Spatial-FISH company (Kit: SPRFK002001). The sequences for detecting *Tad_60482* gene expression were listed in Supplementary Table 1. Staining images were acquired with an LSM900 (Zeiss) confocal microscope.

Recording of ciliary movement

The animals were placed in a confocal petri dish filled with 1 ml of ASW. To label the cilia, a cellmask (Thermo Fisher) was added at a ratio of 1:500. Following a 30-minute incubation period, the medium was exchanged with fresh seawater, and incubation continued for an additional 10 min. The ciliary beating was then recorded using a spinning-disk confocal imaging system (Andor). Cilia movement was captured at a rate of 50 frames per second, and playback was set at 15 frames per second. Image processing was performed using ImageJ software (National Institutes of Health, Bethesda, MD, USA). For each cilium, the beating direction was analyzed frame-by-frame, and the results were graphed using Adobe Illustrator.

Gene knockdown strategy

For gene knockdown analysis, we employed a short hairpin RNAs (shRNAs) mediated knockdown approach. Initially, approximately 30 animals were selected from the culture medium and incubated in fresh seawater for 2 h. These animals were subsequently transferred into a 24-well plate, with each well containing approximately 390 μ l of seawater. Around 2-4 μ g of shRNA (single or mixture of three targeting shRNA) were then incubated with 10 μ l of 10 μ g/ μ l homemade spike silica nanoparticles (SSN) for 15 min at room temperature. Afterward, the mixture was added to each well containing the animals and incubated for 24 hours in darkness. Following the incubation period, the animals were transferred back into regular seawater and fed with algae for another 6 to 12 hours. Subsequently, either qPCR analysis or drug treatment experiments were performed. In some instances, we

extended the incubation time of SSN, which led to an improvement in the transfection efficiency. The design and synthesis of shRNA were conducted as previously described⁵⁶, and sequences were listed in Supplementary Table 2.

For FuGENE6 transfection experiments, 6 μ l FuGENE6 (Promega) was mixed with 2-4 μ g shRNA at RT for 15 min before transfection. The other conditions were similar to the above SSN transfection experiment.

Gene expression analysis

Total RNA was isolated using RNA isolation Kit-BOX2 (Vazyme) from around 20 animals. Reverse transcription was performed using the HiScript III 1st Strand cDNA Synthesis Kit (Vazyme), and the ChamQ Universal SYBR qPCR Master Mix (Vazyme) was used to monitor DNA synthesis. The expression of the *Trichoplax ef1 α* gene (*Tad_XP_002117044.1*) was used as an internal control. Each experiment was repeated at least three times.

Electric shock and ELISA experiment

To test *Trichoplax*'s response to electrical stimulation, we developed a homemade device. This device utilized the Arduino UNO R3 microcontroller to generate a stable rectangular pulse with a specific duration and duty cycle. The pulse duration and delay were set to 50 ms through a program that continuously cycled on the controller. To control the voltage of electrical stimulation at ~100 mV, we employed a potentiometer as a voltage divider. Metal electrodes were then positioned on both sides of the *Trichoplax*, maintaining a distance of around 1 mm. For the control group, the electrodes remained disconnected from the controller. The process of behavior recording was similar to the one mentioned earlier.

Regarding ELISA analysis, we collected six batches of 80 individuals in each group. Epinephrine content was measured using an epinephrine alpha-receptor ELISA kit from MLbio (ML485270V). We also utilized PBS, *Rhodomonas salina* (food of *Trichoplax*), *Paramecium caudatum*, and *Euplotes vannus* as negative controls and zebrafish brain extracts as positive controls. For brain dissection, adult zebrafish were first euthanized using tricaine in ice-cold water, and then their skulls were removed with tweezers in 1X PBS to expose the brain. The dissected brain tissue was homogenized using ultrasonic disruption, and the homogenized tissue was stored at -80 °C for further analysis.

RNA-seq analysis

The scRNA-seq data was downloaded from Mendeley Data: 10.17632/bbpkbx968s.2. Seurat 5.0.1 was used to cluster cells with the parameters (dims = 1:10, resolution = 0.5) after data cleaning in R 4.3.2. The Uniform Manifold Approximation and Projection (UMAP) method was then used to visualize clustering distances. Markers were identified using the FindAllMarkers function and subsequently used for cluster annotation.

We checked the quality of the RNA-seq reads for each sample using FastQC v0.9.7 and aligned the reads with the reference genome using STAR v2.7.6a. FeatureCounts was used to report read counts and transcripts per million (TPM) were calculated using R software.

Reporting summary

Further information on research design is available in the Nature Portfolio Reporting Summary linked to this article.

Data availability

The reanalysis of the scRNA-seq data and gene phylogenetic trees are available at Figshare (10.6084/m9.figshare.26798683). Data supporting the findings of this work are available within the paper and the Supplementary Information files/Source Data file. Additional data that support the findings of this study are also available from the corresponding author upon request. Source data are provided in this paper.

Code availability

All code to generate the single-cell atlases is available at Figshare (10.6084/m9.figshare.26798683). Unless otherwise specified, scripts are based on R version 4.3.2 and Python version 3.2.2.

References

1. Singer, S. J. Intercellular communication and cell-cell adhesion. *Science* **255**, 1671–1677 (1992).
2. Armingol, E., Officer, A., Harismendy, O. & Lewis, N. E. Deciphering cell-cell interactions and communication from gene expression. *Nat. Rev. Genet.* **22**, 71–88 (2021).
3. Budd, G. E. Early animal evolution and the origins of nervous systems. *Philos. Trans. R. Soc. B Biol. Sci.* **370**, <https://doi.org/10.1098/rstb.2015.0037> (2015).
4. Hartenstein, V. & Stollewerk, A. The evolution of early neurogenesis. *Dev. Cell* **32**, 390–407 (2015).
5. Moroz, L. L. et al. The ctenophore genome and the evolutionary origins of neural systems. *Nature* **510**, 109–114 (2014).
6. Schultz, D. T. et al. Ancient gene linkages support ctenophores as sister to other animals. *Nature* **618**, 110–117 (2023).
7. Ryan, J. F. et al. The genome of the ctenophore *Mnemiopsis leidyi* and its implications for cell type evolution. *Science* **342**, 1242592 (2013).
8. Burkhardt, P. et al. Syncytial nerve net in a ctenophore adds insights on the evolution of nervous systems. *Science* **380**, 293–297 (2023).
9. Arendt, D., Tosches, M. A. & Marlow, H. From nerve net to nerve ring, nerve cord and brain-evolution of the nervous system. *Nat. Rev. Neurosci.* **17**, 61–72 (2016).
10. Sachkova, M. Y. Evolutionary origin of the nervous system from Ctenophora prospective. *Evol. Dev.* **26**, e12472 (2024).
11. Ryan, J. F. & Chiodin, M. Where is my mind? How sponges and placozoans may have lost neural cell types. *Philos. Trans. R. Soc. B Biol. Sci.* **370**, 20150059 (2015).
12. Elliott, G. R. & Leys, S. P. Evidence for glutamate, GABA and NO in coordinating behaviour in the sponge, *Ephydatia muelleri* (Demospongiae, Spongillidae). *J. Exp. Biol.* **213**, 2310–2321 (2010).
13. Fortunato, A. & Aktipis, A. Social feeding behavior of Trichoplax adhaerens. *Front. Ecol. Evol.* **7**, <https://doi.org/10.3389/fevo.2019.00019> (2019).
14. Schierwater, B. et al. The enigmatic Placozoa part 1: Exploring evolutionary controversies and poor ecological knowledge. *Bioessays* **43**, e2100080 (2021).
15. Srivastava, M. et al. The Trichoplax genome and the nature of placozoans. *Nature* **454**, 955–960 (2008).
16. Smith, C. L. et al. Novel cell types, neurosecretory cells, and body plan of the early-diverging metazoan Trichoplax adhaerens. *Curr. Biol.* **24**, 1565–1572 (2014).
17. Mayorova, T. D., Hammar, K., Winters, C. A., Reese, T. S. & Smith, C. L. The ventral epithelium of Trichoplax adhaerens deploys in distinct patterns cells that secrete digestive enzymes, mucus or diverse neuropeptides. *Biol. Open* **8**, bio045674 (2019).
18. Mayorova, T. D. et al. Cells containing aragonite crystals mediate responses to gravity in Trichoplax adhaerens (Placozoa), an animal lacking neurons and synapses. *PLoS ONE* **13**, e0190905 (2018).
19. Romanova, D. Y. et al. Hidden cell diversity in Placozoa: ultrastructural insights from *Hoilungia hongkongensis*. *Cell Tissue Res.* **385**, 623–637 (2021).
20. Sebe-Pedros, A. et al. Early metazoan cell type diversity and the evolution of multicellular gene regulation. *Nat. Ecol. Evol.* **2**, 1176–1188 (2018).
21. Najle, S. R. et al. Stepwise emergence of the neuronal gene expression program in early animal evolution. *Cell* **186**, 4676–4693 e4629 (2023).
22. Davidescu, M. R., Romanczuk, P., Gregor, T. & Couzin, I. D. Growth produces coordination trade-offs in Trichoplax adhaerens, an animal lacking a central nervous system. *Proc. Natl. Acad. Sci. USA* **120**, e2206163120 (2023).
23. Smith, C. L., Reese, T. S., Govezensky, T. & Barrio, R. A. Coherent directed movement toward food modeled in Trichoplax, a ciliated animal lacking a nervous system. *Proc. Natl. Acad. Sci. USA* **116**, 8901–8908 (2019).
24. Smith, C. L., Pivovarova, N. & Reese, T. S. Coordinated Feeding Behavior in Trichoplax, an Animal without Synapses. *PLoS ONE* **10**, e0136098 (2015).
25. Senatore, A., Reese, T. S. & Smith, C. L. Neuropeptidergic integration of behavior in Trichoplax adhaerens, an animal without synapses. *J. Exp. Biol.* **220**, 3381–3390 (2017).
26. Varoqueaux, F. et al. High cell diversity and complex peptidergic signaling underlie placozoan behavior. *Curr. Biol.* **28**, 3495–3501 e3492 (2018).
27. Armon, S., Bull, M. S., Aranda-Diaz, A. & Prakash, M. Ultrafast epithelial contractions provide insights into contraction speed limits and tissue integrity. *Proc. Natl. Acad. Sci. USA* **115**, E10333–E10341 (2018).
28. Moroz, L. L. & Kohn, A. B. Unbiased view of synaptic and neuronal gene complement in ctenophores: Are there pan-neuronal and pan-synaptic genes across metazoa? *Integr. Comp. Biol.* **55**, 1028–1049 (2015).
29. Moroz, L. L., Romanova, D. Y. & Kohn, A. B. Neural versus alternative integrative systems: molecular insights into origins of neurotransmitters. *Philos. Trans. R. Soc. B Biol. Sci.* **376**, 20190762 (2021).
30. Romanova, D. Y. et al. Glycine as a signaling molecule and chemoaattractant in Trichoplax (Placozoa): insights into the early evolution of neurotransmitters. *Neuroreport* **31**, 490–497 (2020).
31. Kamm, K., Osigus, H. J., Stadler, P. F., DeSalle, R. & Schierwater, B. Trichoplax genomes reveal profound admixture and suggest stable wild populations without bisexual reproduction. *Sci Rep* **8**, 11168 (2018).
32. Fortunato, A., Fleming, A., Aktipis, A. & Maley, C. C. Upregulation of DNA repair genes and cell extrusion underpin the remarkable radiation resistance of Trichoplax adhaerens. *PLoS Biol.* **19**, e3001471 (2021).
33. Zhang, P. et al. On the origin and evolution of RNA editing in metazoans. *Cell Rep.* **42**, 112112 (2023).
34. Fu, J. et al. Silica nanoparticles with virus-mimetic spikes enable efficient siRNA delivery in vitro and in vivo. *Research* **2022**, <https://doi.org/10.34133/research.0014> (2022).
35. Heidari, R., Khosravian, P., Mirzaei, S. A. & Elahian, F. siRNA delivery using intelligent chitosan-capped mesoporous silica nanoparticles for overcoming multidrug resistance in malignant carcinoma cells. *Sci. Rep.* **11**, 20531 (2021).
36. Chen, J., Wang, Y., Wu, C., Xiao, Y. & Zhu, Y. A coronavirus-mimic mesoporous silica nanosystem enables efficient targeted delivery of siRNA for anti-SARS-CoV-2. *Appl. Mater. Today* **35**, <https://doi.org/10.1016/j.apmt.2023.101952> (2023).
37. Jakob, W. et al. The *Trox-2* Hox/ParaHox gene of Trichoplax (Placozoa) marks an epithelial boundary. *Dev. Genes Evol.* **214**, 170–175 (2004).
38. Zhao, L. et al. Heme-binding protein CYB5D1 is a radial spoke component required for coordinated ciliary beating. *Proc. Natl. Acad. Sci. USA* **118**, e2015689118 (2021).
39. Tang, D. et al. Morpholino-mediated knockdown of ciliary genes in *Euplotes vannus*, a novel marine ciliated model organism. *Front. Microbiol.* **11**, 549781 (2020).
40. Gruber-Vodicka, H. R. et al. Two intracellular and cell type-specific bacterial symbionts in the placozoan Trichoplax H2. *Nat. Microbiol.* **4**, 1465–1474 (2019).
41. Mayorova, T. D. et al. Placozoan fiber cells: mediators of innate immunity and participants in wound healing. *Sci. Rep.* **11**, 23343 (2021).

42. Smith, C. L. & Reese, T. S. Adherens junctions modulate diffusion between epithelial cells in trichoplax adhaerens. *Biol. Bull.* **231**, 216–224 (2016).
43. Roy, S., Huang, H., Liu, S. & Kornberg, T. B. Cytoneme-mediated contact-dependent transport of the Drosophila decapentaplegic signaling protein. *Science* **343**, 1244624 (2014).
44. Huang, H., Liu, S. & Kornberg, T. B. Glutamate signaling at cytoneme synapses. *Science* **363**, 948–955 (2019).
45. Hall, E. T. et al. Cytoneme signaling provides essential contributions to mammalian tissue patterning. *Cell* **187**, 276–293 (2024).
46. Zhang, C., Brunt, L., Ono, Y., Rogers, S. & Scholpp, S. Cytoneme-mediated transport of active Wnt5b-Ror2 complexes in zebrafish. *Nature* **625**, 126–133 (2024).
47. Gouley, M., Botton-Amiot, G., Rosato, E., Sprecher, S. G. & Feuda, R. The monoaminergic system is a bilaterian innovation. *Nat. Commun.* **14**, 3284 (2023).
48. Kolberg, K. J. & Martin, V. J. Morphological, cytochemical and neuropharmacological evidence for the presence of catecholamines in hydrozoan planulae. *Development* **103**, 249–258 (1988).
49. Walker, R. J., Brooks, H. L. & Holden-Dye, L. Evolution and overview of classical transmitter molecules and their receptors. *Parasitology* **113**, S3–S33 (1996).
50. Mathias, A. P., Ross, D. M. & Schachter, M. The distribution 5-hydroxytryptamine, tetramethylammonium, homarine, and other substances in sea anemones. *J. Physiol.* **151**, 296–311 (1960).
51. Umbriaco, D., Anctil, M. & Descarries, L. Serotonin-immunoreactive neurons in the cnidarian Renilla koellikeri. *J. Comp. Neurol.* **291**, 167–178 (1990).
52. Mayorova, T. D. & Kosevich, I. A. Serotonin-immunoreactive neural system and contractile system in the hydroid Cladonema (Cnidaria, Hydrozoa). *Invert. Neurosci.* **13**, 99–106 (2013).
53. Chan, I. Z. W., Stevens, M. & Todd, P. A. pat-geom: A software package for the analysis of animal patterns. *Methods Ecol. Evol.* **10**, 591–600 (2019).
54. Katoh, K., Rozewicki, J. & Yamada, K. D. MAFFT online service: multiple sequence alignment, interactive sequence choice and visualization. *Brief. Bioinform.* **20**, 1160–1166 (2019).
55. Tao, Y. et al. Highly efficient and robust pi-FISH rainbow for multiplexed *in situ* detection of diverse biomolecules. *Nat. Commun.* **14**, 443 (2023).
56. Karabulut, A., He, S., Chen, C. Y., McKinney, S. A. & Gibson, M. C. Electroporation of short hairpin RNAs for rapid and efficient gene knockdown in the starlet sea anemone, *Nematostella vectensis*. *Dev. Biol.* **448**, 7–15 (2019).
57. Krishnan, A. & Schiøth, H. B. The role of G protein-coupled receptors in the early evolution of neurotransmission and the nervous system. *J. Exp. Biol.* **218**, 562–571 (2015).
58. Nordstrom, K. J., Sallman Almen, M., Edstam, M. M., Fredriksson, R. & Schiøth, H. B. Independent HHsearch, Needleman-Wunsch-based, and motif analyses reveal the overall hierarchy for most of the G protein-coupled receptor families. *Mol. Biol. Evol.* **28**, 2471–2480 (2011).
59. Krishnan, A. et al. The GPCR repertoire in the demosponge *Amphimedon queenslandica*: insights into the GPCR system at the early divergence of animals. *BMC Evol. Biol.* **14**, 270 (2014).

Acknowledgements

We thank Drs. Leo Buss (Yale University) and Carolyn L. Smith (National Institutes of Health) for providing us with *Trichoplax adhaerens* and red

algae strain *Rhodomonas salina* and Prof. Shichun Sun, Ms. Xiujuan Hu for the help during acquiring an initial culture of *Trichoplax adhaerens* and *Rhodomonas salina*. We thank Drs. Bo Dong, Shi Wang, Wei Wang, Li Yu, Xiaozhi Rong, Meng Qiu, Xin Wang, Yuanning Li, and Kai Chen, for their kind help during the preparation of this manuscript. We are also grateful for the excellent support from the core facilities of IEMB and the FANG center at OUC. This work was supported by the National Natural Science Foundation of China (Nos. 32125015, 31991194 to C.Z. and No. 32200415 to Y.K.), funds from Laoshan Laboratory (LSKJ202203204), and the Fundamental Research Funds for Central Universities of China (Grant 202064009) to C.Z.

Author contributions

C.Z. and M.J. conceived the idea for the project. C.Z. and M.J. designed the experiments. M.J., W.L., Z.J., and G.D. conducted the experiments. M.J., W.L., Y.Z., M.Y., and Y.K. analyzed the results. C.Z. and M.J. wrote the paper. All authors reviewed the results and approved the final version of the manuscript.

Competing interests

The authors declare no competing interests.

Additional information

Supplementary information The online version contains supplementary material available at <https://doi.org/10.1038/s41467-024-52941-y>.

Correspondence and requests for materials should be addressed to Chengtian Zhao.

Peer review information *Nature Communications* thanks the anonymous reviewers for their contribution to the peer review of this work. A peer review file is available.

Reprints and permissions information is available at <http://www.nature.com/reprints>

Publisher's note Springer Nature remains neutral with regard to jurisdictional claims in published maps and institutional affiliations.

Open Access This article is licensed under a Creative Commons Attribution-NonCommercial-NoDerivatives 4.0 International License, which permits any non-commercial use, sharing, distribution and reproduction in any medium or format, as long as you give appropriate credit to the original author(s) and the source, provide a link to the Creative Commons licence, and indicate if you modified the licensed material. You do not have permission under this licence to share adapted material derived from this article or parts of it. The images or other third party material in this article are included in the article's Creative Commons licence, unless indicated otherwise in a credit line to the material. If material is not included in the article's Creative Commons licence and your intended use is not permitted by statutory regulation or exceeds the permitted use, you will need to obtain permission directly from the copyright holder. To view a copy of this licence, visit <http://creativecommons.org/licenses/by-nc-nd/4.0/>.

© The Author(s) 2024